



1  
2

## Probabilistic Fault Displacement Hazard Analysis for North Tabriz Fault

3

Mohamadreza Hosseyni<sup>1</sup>, Habib Rahimi,<sup>2</sup>

4

*1. M.Sc. Graduated, Department of Earth Physics, Institute of Geophysics, University of Tehran, Tehran, Iran*

5

*2. Associate Professor, Department of Earth Physics, Institute of Geophysics, University of Tehran, Tehran, Iran*

6

*Corresponding author: Habib Rahimi; email: [rahimih@ut.ac.ir](mailto:rahimih@ut.ac.ir)*

7

### 8 **Abstract:**

9 The probabilistic fault displacement hazard analysis is one of the new methods in estimating the amount of possible  
10 displacement in the area at the hazard of causal fault rupture. In this study, using the probabilistic approach and  
11 earthquake method introduced by Youngs et al., 2003, the surface displacement of the North Tabriz fault has been  
12 investigated, and the possible displacement in different scenarios has been estimated. By considering the strike-slip  
13 mechanism of the North Tabriz fault and using the earthquake method, the probability of displacement due to surface  
14 ruptures caused by 1721 and 1780 North Tabriz fault earthquakes has been explored. These events were associated  
15 with 50 and 60 km of surface rupture, respectively. The 50-60 km long section of the North Tabriz fault was selected  
16 as the source of possible surface rupture.

17 We considered two scenarios according to possible displacements, return periods, and magnitudes which are reported  
18 in paleoseismic studies of the North Tabriz fault. As the first scenario, possible displacement, return period, and  
19 magnitude was selected between zero to 4.5; 645 years and  $M_w \sim 7.7$ , respectively. In the second scenario, possible  
20 displacement, return period and magnitude were selected between zero to 7.1, 300 years, and  $M_w \sim 7.3$ , respectively.  
21 For both mentioned scenarios, the probabilistic displacements for the rate of exceedance 5% in 50, 475, and 2475  
22 years for the principle possible displacements (on fault) of the North Tabriz fault have been estimated. For the first  
23 and second scenarios, the maximum probabilistic displacement of the North Tabriz fault at a rate of 5% in 50 years is  
24 estimated to be 186 and 230 cm. Also, mentioned displacements for 5% exceedance in 475 years and 2475 years in  
25 both return periods of 645 and 300 years, are estimated at 469 and 655cm.

26 **Keywords:** Surface rupture, Hazard, probabilistic fault displacement, North Tabriz fault, Iran.

27

### 28 **1- Introduction**

29 Earthquakes, not only because of earth-shaking but also because of surface ruptures, are a serious threat to many  
30 human activities. Reducing earthquake losses and damages requires predicting the amplitude and location of ground  
31 movements and possible surface displacements in the future. Fault displacement hazard assessments are based on  
32 empirical relationships obtained using historical seismic rupture data. These relationships evaluate the probability of  
33 co-seismic surface slip of ruptures on fault (primary) and outside the fault (distributed) for different magnitudes and



34 distances to the causal fault. In addition, these relationships make it possible to predict the extent of fault slip on or  
35 near the active fault (Stephanie Baiz et al., 2019).

36 A way to reduce the effects of fault rupture hazards on a structure is to develop the probability of fault  
37 displacement. This approach can be taken into account the rate of exceedance of different displacement levels of the  
38 event under a structure, along with a displacement hazard curve (Youngs et al., 2003). In surface displacement hazard  
39 studies, non-tectonic displacements such as fault creep, aftershock, soil liquefaction, and landslide are not considered  
40 (Petersen et al., 2011). So far, fault displacement data have been collected and analyzed by several researchers to  
41 evaluate the fault rupture properties. Investigation of fault displacement and extraction of experimental relationships  
42 between rupture length and magnitude, rupture length and fault mechanism, maximum fault displacement, average  
43 fault displacement, and other cases are investigated by Wells and Coppersmith (1993 and 1994) and reviewed by  
44 Petersen and Wesnousky (1994). To be considered, each earthquake causes a superficial shaking at the site, but each  
45 earthquake does not cause a surface rupture in the area. Therefore, only the data of earthquakes that have caused the  
46 rupture in the region are used to obtain the attenuation relationships (Youngs et al., 2003). Principal displacements are  
47 considered primary ruptures that occur on or within a few meters of the active fault. Distributed displacements outside  
48 the fault are causative and usually appear as discontinuous ruptures or shears distance several meters to several  
49 hundred kilometers from the fault trace. The principal and distributed displacements are introduced as net  
50 displacements derived from horizontal and vertical displacements (Petersen et al., 2011).

51 A method for estimating the probabilistic fault displacement hazard for strike-slip faults in the world has been  
52 presented, mapped due to the impact of fault displacement hazard to the fault trace type and the complexity of this  
53 effect and hazard of fault displacement for strike-slip faults studied (Petersen et al., 2011). The North Tabriz fault has  
54 a high level of danger by passing through the 5th district of Tabriz city, and in case of possible surface rupture, it will  
55 lead to many damages in this residential area. With 150,000 people and 32,000 square kilometers, this region has  
56 essential areas such as Baghmisheh, Elahieh, Rashidieh town, etc. (Figure 1).

57 In this study, based on the results of a paleoseismic study reported by Hesami et al. (2003) on the North Tabriz fault,  
58 the section with a length of 50 - 60 km was considered as a source of possible rupture in the future. To describe the  
59 possible behavior of the displacement rupture hazard of the North Tabriz fault, sites at distances of 50 m from each  
60 other and cells with dimensions of  $25 \times 25$  m<sup>2</sup> on fault trace were considered, which is shown in Figures 1. Also,  
61 according to the study of Petersen et al. (2011), the trace of the North Tabriz fault was considered as a simple trace  
62 due to the absence of large instrumental earthquakes that are associated with surface rupture. Many studies have been  
63 done on the historical displacements of the North Tabriz fault. According to the results of paleoseismic studies reported  
64 by Hesami et al. (2003) and Ghasemi et al. (2015), the probabilistic displacement is between zero to 4.5 and zero to  
65 7.1 m, respectively. The magnitude and return period of large earthquakes are considered 645 years with  $M_w \sim 7.7$   
66 and 300 years with  $M_w \sim 7.3$  according to Mousavi et al. 2014 and Dejamour et al., 2011, respectively.

67 In this study and the first step, probabilistic fault displacement and annual rate of exceedance of displacement for two  
68 given scenarios (645 years with  $M_w \sim 7.7$ ) and (300 years with  $M_w \sim 7.3$ ) have been achieved by considering 5%  
69 exceedance rate in 50, 475, and 2475 years at the site with geographical coordinates (38.096, 46.349). In the second



70 step, due to the passage of the North Tabriz Fault through the city of Tabriz, considering a 2 km long section from the  
71 North Tabriz Fault, the probabilistic displacement has been estimated, and the probabilistic displacement 2D map is  
72 explored.

73

74

## 752- Seismotectonic

76 With over two million people and an area of 167 square kilometers in northwestern Iran, Tabriz is one of the  
77 most populated cities in the country that has experienced devastating earthquakes throughout history. One of the main  
78 problems of Tabriz City is the proximity of the city to the North Tabriz fault and the expansion of constructions around  
79 it. Based on the reported historical earthquakes by Berberian and Arshadi (1979), since 858 AD., this city and the  
80 surrounding area have experienced several large and medium destructive earthquakes.

81 The focal mechanism of earthquakes in northwestern Iran and southeastern Turkey shows that the convergence  
82 between the Saudi and Eurasian plates becomes depreciable during right-lateral strike-slip faults. The strike-slip fault  
83 is the southeastern continuation of the North Anatolian Fault into Iran, consisting of discontinuous fault sections with  
84 a northwest-southeast extension (Jackson and Mackenzie et al., 1992). Some of these fault fragments have been  
85 ruptured and left deformed along with the earthquakes in 1930, 1966, and 1976 (Hesami et al., 2003).

86 Nevertheless, the North Tabriz fault is one of the components of this right-lateral strike-slip system, which has not  
87 had a major earthquake during the last two centuries. Among the many historical earthquakes in the Tabriz region,  
88 only three devastating earthquakes with a magnitude of  $M_s \sim 7.3$  in 1042, 1721, and 1780 with a magnitude of  $M_s \sim 7.4$   
89 had been associated with a surface rupture along the North Tabriz fault (Hesami et al., 2003). The 1721 and 1780 AD  
90 earthquakes were along with at least 50 and 60 km of surface rupture (about 40 km overlap), respectively. Berberian  
91 et al., 1997 believe that large earthquakes along the North Tabriz fault are concentrated at specific times and spatially  
92 related.

93 The occurrence of the 1976 Chaldoran earthquake in Turkey, which was accompanied by about 55 km of fractures,  
94 indicates that the length of the surface fracture caused by historical earthquakes in this region probably varies from  
95 about 50 to 60 km (Toxos et al., 1977). A more detailed study of the temporal distribution of earthquakes in Tabriz by  
96 Berberian and Yates (1999) also shows the cluster distribution of earthquakes over time. Due to the absence of seismic  
97 events for more than 200 years in the Tabriz area (decluttering period), the study area has passed the final stages of  
98 stress storage, and it is ready to release the stored energy. Therefore, Hesami et al., 2003 investigated the Spatial-  
99 temporal concentration of earthquakes associated with the North Tabriz fault. Based on paleontological seismic studies  
100 on the western part of the North Tabriz fault, Hesami et al., 2003 introduced four earthquakes that occurred  
101 continuously on the western part of the North Tabriz fault. The return periods of these earthquakes were suggested to  
102 be  $821 \pm 176$  years. The amount of right-lateral strike-slip displacement, during each seismic event, of the North  
103 Tabriz fault, has been estimated at 3.5 to 4.5 m. In addition, Berberian et al., 1997 considered the possibility of



104 fracturing all parts of the North Tabriz fault at once and mentioned it as one of the critical issues in the earthquake  
105 hazard for the Tabriz city and the northwestern region of Iran.

106

### 1073- Methodology of probabilistic fault displacement hazard analysis

108 Probabilistic seismic hazard analysis has been used since its development in the late 1960s and early 1970s  
109 to assess shaking hazards and to establish seismic design parameters (Cornell, 1968 and 1971). A method for analyzing  
110 the hazard of probabilistic fault displacement was introduced in two approaches of earthquake and displacement  
111 (Youngs et al., 2003). This method was first proposed to estimate the displacement of Yucca Mountain faults, which  
112 were the landfill of nuclear waste (Stepp et al., 2001). Then, the probabilistic fault displacement hazard analysis  
113 method was introduced for an environment with normal faults, and the probability distributions obtained for each type  
114 of fault in the world can be used in areas with similar tectonics (Youngs et al., 2003).

115 The earthquake approach is similar to the analysis of probabilistic seismic hazard related to displacement, features  
116 such as faults, partial shear, fracture, or unbroken ground at or near the ground surface so that the attenuation  
117 relationships of the fault displacement replace the ground shaking relationships. In the displacement approach, without  
118 examining the rupture mechanism, the displacement characteristics of the fault observed at the site are used to  
119 determine the hazard in that area.

120 The occurrence rate of displacements and the distribution of fault displacements are obtained directly from the fault  
121 characteristics of geological features (Youngs et al., 2003). To calculate the rate of exceedance in the earthquake  
122 approach, similar to probabilistic seismic hazard analysis relationships were used. The rate of exceedance,  $v_k(z)$ , is  
123 calculated according to the Cornell relationship (1968 and 1971) as follows (Youngs et al., 2003):

124

$$v_k(z) = \sum_n \alpha_n (m^0) \int_{m^0}^{m_n^u} f_n(m) \left[ \int_0^\infty f_{kn}(r|m) \cdot P^*(Z > z/m, r) \cdot dr \right] \cdot dm \quad (1)$$

125 In which the ground motion parameter,  $(Z)$ , (maximum ground acceleration, maximum response spectral acceleration)  
126 exceed the specified level  $(z)$  at the site  $(k)$ . Considering Equation (1) and to calculate the exceedance rate of  
127 displacement  $(D)$  from a specific value  $(d)$ , the displacement parameter replaces the parameters of ground motion  
128 (Youngs et al., 2003):

$$v_k(d) = \sum_n \alpha_n (m^0) \int_{m^0}^{m_n^u} f_n(m) \left[ \int_0^\infty f_{kn}(r|m) \cdot P^*(D > d/m, r) \cdot dr \right] \cdot dm \quad (2)$$

129 The expression  $P(D > d|m, r)$  is the "attenuation function" of the fault displacement at or near the earth's surface. This  
130 displacement attenuation function is different from the usual ground motion attenuation function and includes the  
131 multiplication of the following two probabilities (Youngs et al., 2003):

$$P_{kn}^*(D > d|m, r) = P_{kn}(Slip|m, r) \cdot P_{kn}(D > d|m, r, slip) \quad (3)$$

132 Which  $D$  and  $d$  are the Displacement on fault (principal fault) and displacement on the outside of the fault (distributed  
133 fault), respectively.  $(x, y)$  are considered as coordinates of the site.  $r, z^2, I, L$ , and  $s$  are the vertical distance from the



134 fault, area, the distance of site on fault rupture to the nearest rupture, the total length of the fault surface rupture, and  
135 the rupture distance to the end of the fault, respectively. The definition of these variables is shown in figure (2).  
136 The following Equation has been used to obtain the exceedance rate of probabilistic displacement due to the principal  
137 fault (on fault) (Petersen et al., 2011):

$$\lambda(D \geq D_0)xyz = \quad (4)$$

$$\alpha(m) \int_{m,s} f_{M,s}(m, s) P[sr \neq 0|m] * \int_r P[D \neq 0|z, sr \neq 0] * P[D \geq D_0 | l/L, m, D \neq 0] f_R(r) dr dms$$

138 The magnitude of the earthquake is indicated by  $m$ . In relation 4 and to assess the displacement hazard due to fault  
139 rupture, the probability density functions that describe displacement potential due to earthquakes on or near a rupture,  
140 as well as the probabilities that the potential for non-zero ruptures are used (Petersen et al., 2011). In the following,  
141 each of the parameters for estimation of probabilistic fault displacement hazard is described.

### 142 3-1 Probability density function

143 The probability density function  $f_{M,s}(m, s)$  determines the magnitude of the earthquake and the location of  
144 the ruptures on a fault. Since the magnitude and the rupture position on the causal fault are correlated, a probabilistic  
145 distribution is used to calculate these parameters. In the next step, the variability in the rupture location is considered.  
146 A probability density function  $f_R(r)$  is considered to define the area of perpendicular distances ( $r$ ) to the site to different  
147 potential ruptures (Petersen et al., 2011).

### 148 3-2 Probabilities

149 Probability  $P[SR \neq 0 | M]$  is the ratio of cells with rupture on the principal fault to the total number of cells  
150 considered. Therefore, the probability of surface rupture  $P[SR \neq 0 | M]$  is considered due to a certain magnitude  $M$   
151 due to faulting. According to studies of Wells and Coppersmith (1993), due to the formulation of empirical  
152 relationships between different fault parameters, probability has been obtained for different faults in the world, such  
153 as strike-slip, normal, and revers. Therefore, in hazard analysis of fault displacement, it is necessary to investigate the  
154 possibility of surface rupture with magnitude ( $M$ ) on the ground so as a result, the equation (5) introduced by Wells  
155 and Coppersmith (1993) can be used. According to this relation, the coefficients  $a$  and  $b$  are constant, and strike-slip  
156 faults with -12.51 and 2.553 have been reported. This relationship has a 10% probability for the size of  $M_w \sim 5$  and a  
157 95% probability of surface rupture for a magnitude of  $M_w \sim 7.5$  ((Rizzo et al., 2011).

158

$$P[sr \neq 0|m] = \frac{e^{a+bm}}{1+e^{a+bm}} \quad (5)$$

159 This rupture probability was used to estimate the exceedance rate of displacement because of earthquakes such as  
160 Loma-Prieta in 1989 with a magnitude of  $M_w \sim 6.9$  and Alaska in 2002 with a magnitude of  $M_w \sim 6.7$ . These  
161 earthquakes did not cause rupture to reach the earth's surface. Therefore, these two earthquakes did not cause surface



162 deformation and are considered non-tectonic phenomena (Petersen et al., 2011). The expression  $P[D \neq 0|z, sr \neq 0]$   
163 indicates the probability of non-zero displacement at a distance  $r$  from the rupture in an area of size  $z^2$  and due to the  
164 magnitude event  $m$  associated with the surface rupture. The probability  $P[D \geq D_0 | l/L, m, D \neq 0]$  for displacements  
165 more significant than or equal to the value given at this site is intended for the principal displacement (on fault). This  
166 probability is obtained by integrating around a log-normal distribution (Petersen et al., 2011).

167

### 168 **3-3 Rate parameter $\alpha(m)$ :**

169 When the potential magnitude of an earthquake with a certain magnitude is modeled, it is possible to estimate how  
170 often these ruptures occur. The,  $\alpha(m)$ , rate parameter used describes the frequency of repetition of these earthquakes  
171 in this model. This parameter is a function of magnitude and can only function as a single rupture function or a function  
172 of cumulative earthquakes above the magnitude of the minimum importance in engineering projects (Youngs et al.,  
173 2003). This parameter is usually based on slip rate, paleoseismic rate of large earthquakes, or historical fault rate  
174 earthquakes and is described in earthquake units per year. By removing the  $\alpha(m)$  parameter from Equation (4), the  
175 Deterministic Fault Displacement Hazard can be estimated (Petersen et al., 2011).

176

### 177 **3-4 Cell size:**

178 In calculating the hazard of principal fault displacements, as shown in Eq. (4), by changing the size of the cells, the  
179 level of hazard will not change and this parameter can be examined by the availability of principal displacement data  
180 in the study area. In calculating the hazard of distributed rupture (distributed displacement), considering the method  
181 of Youngs et al. (2003), by modeling secondary displacements up to a distance of 12 km from the fault, the probability  
182 of surface rupture was investigated. According to studies by Petersen (2011), the relationship between the calculations  
183 of the probability of rupture of the principal faults (5), in calculating the probability of rupture of the distributed faults  
184 became the following relationship (Petersen et al., 2011):

185

$$\text{Ln}(p) = a(z) \ln(r) + b(z) \quad (6)$$

186 The values of the coefficients used for the cell sizes of  $25 \times 25$  to  $200 \times 200$  m<sup>2</sup> in the above relationship are given in  
187 Table 1 (Petersen et al., 2011).

188

### 189 **3-5 Surveying accuracy**

190 The accuracy of fault location is a function of geological and geomorphic conditions that play an essential  
191 role in diagnosing and interpreting a geologist in converting this spatial information into geological maps and fault  
192 geographic information systems. A fault map is generated using aerial photography imagery, interpretation of fault  
193 patterns from geomorphology, and conversion of fault locations into a base map. In many cases, identifying the  
194 location and trace of the fault may be difficult because sediments and erosion may obscure or cover the fault surface,  
195 leading to more uncertainty in identifying the actual location of the fault. Therefore, trace mapped faults are divided  
196 into four categories: accurate, approximate, inferred, and concealed, based on how clearly and precisely they are  
197 located (Petersen et al., 2011).



198 A practical example shows that an active fault with large earthquakes repeated over several hundred years, fault  
199 rupture hazard analysis should be one of the critical topics considered for the design of structures or pipelines that are  
200 close to this fault, and if this the fault has a complex or straightforward trace, avoiding the fault from the constructor  
201 to a distance of 150 and 300 meters, respectively. Table 2 summarizes the standard deviations for the displacements  
202 observed in strike-slip earthquakes for different classifications of mapping accuracy (Petersen et al., 2011). According  
203 to the exponential values obtained from these fitting equations, the mean displacement will be obtained. The following  
204 Equation has been used to obtain the mean displacement (Petersen et al., 2011):

$$D_{mean} = e^{\mu + \sigma^2/2} \quad (7)$$

205

206

### 207 **3-6 Epistemic and Aleatory uncertainty**

208 There are uncertainties about the quality of mapping and the complexity of the fault trace that lead to epistemic  
209 uncertainty at the site of future faults. The probability density function for  $r$  includes both epistemic and aleatory  
210 components. Displacements on and off the principal fault can include components of epistemic uncertainty and  
211 random variability. Epistemic uncertainty is related to displacement measurement errors along fault rupture. Random  
212 variability is related to the natural variability in fault displacements between earthquakes. However, the measured  
213 variability in ruptures involves epistemic mapping uncertainties because there is currently no data to separate these  
214 uncertainties. In addition, epistemic uncertainty of location is introduced due to limitations in the accuracy of basic  
215 maps or images and the accuracy of the equipment used to transfer this information to the map or database (Petersen  
216 et al., 2011).

### 217 **3-7 Attenuation relationship of strike-slip faults**

218 In this study, to estimate the probabilistic displacement of the North Tabriz fault, the attenuation relationship of  
219 Petersen et al. (2011) has been used. The rupture displacement data obtained from the principal fault are scattered but  
220 are generally the most scattered near the fault rupture center and decrease rapidly at the end of the rupture. In some  
221 earthquakes, including the Borgo Mountain earthquake in 1968, the most significant displacement was observed near  
222 the end of the fault surface rupture (Petersen et al., 2011). Many of the collected surface rupture data behave  
223 asymmetrically ruptured (Wesnousky et al., 2008). However, there is currently no way to determine surface rupture  
224 areas that have larger displacements. Thus, the distribution of asymmetric displacements along the length of a fault  
225 will define more considerable uncertainties, especially near the end of the fault rupture (Petersen et al., 2011). To  
226 determine the displacement distribution, the principal fault, two different approaches were introduced by Petersen et  
227 al. (2011). In the first approach, the best-fit equations using the least-squares method related to the natural logarithm  
228 of the displacement ratio of magnitude and distance were developed in a multivariate analysis (Paul Rizzo et al., 2013).  
229 In the second approach, the displacement data is normalized by the average displacement as a distance function. In  
230 normalized analysis, magnitude is not directly considered but influences calculations through the presence of  
231 magnitude in the mean displacement, which is calculated through the studies of Wells and Coppersmith (1994). Three



232 models (bilinear, elliptical and quadratic) were considered to provide the principal fault displacement in multivariate  
233 and normalized analysis (Petersen et al., 2011). However, in multivariate analysis, the three introduced models have  
234 the same aleatory uncertainty, and there is no clear basis for preferring one model to other models. As a result, in the  
235 probabilistic displacement hazard analysis, all three models with the same weights were used according to Table 3.  
236 The results obtained from the multivariate analysis were preferred to the normalized analysis because, in the  
237 normalized analysis, the stochastic uncertainty of calculating the mean displacement from the Wells and Coppersmith  
238 (1994) study is added to the stochastic uncertainty of the results of the Petersen attenuation relationships (Paul Rizzo  
239 et al., 2013). In this study, multivariate analysis and probabilistic displacement estimation have been used in the three  
240 mentioned models. The Equation of the three models is obtained in the multivariate method as shown in Table 3, and  
241 5% uncertainty was considered in the modeling of the strike-slip displacement data (Petersen et al., 2011):  
242

## 243 **4 Results and Discussions**

### 244 **4-1 Probabilistic displacement and rate of exceedance**

245 In the first step, assuming the possible surface rupture of the North Tabriz fault (50 to 60 km), displacement and the  
246 annual exceedance rate are estimated by considering one of the sites located on the Tabriz fault trace related to the  
247 total segment as shown in Figure 1. Considering the return periods of 645 and 300 years, the probabilistic  
248 displacements of the North Tabriz fault are assumed 4.5 and 7.1 m according to Hesami et al. (2003) and Ghasemi et  
249 al. (2015), respectively.

250 Given the 4.5 m probabilistic displacements reported by Hesami et al. (2003), maximum displacement for the return  
251 period of 645 years at an exceedance rate of 5% for 50, 475, and 2475 years are estimated 186, 469, and 469cm,  
252 respectively. The maximum displacement for a return period of 300 years is calculated at 230, 469, and 469cm. These  
253 amounts of displacement were observed for the return period of 645 and 300 years at a distance of 60-100 and 60-80  
254 meters from the selected site respectively, as shown in figure (3a).

255 Also, by considering the 7.1 m probabilistic displacements reported by Ghasemi et al. (2015), maximum displacement  
256 for the return period of 645 years with an exceedance rate of 5% in 50, 475, and 2475 years are estimated 186, 655,  
257 and 655cm, respectively. The maximum displacement for a return period of 300 years is calculated at 230, 655, and  
258 655 cm. These amounts of displacement were observed for the return period of 645 and 300 years at a distance of 60-  
259 80 and 40-80 meters from the selected site respectively, as shown in figure (3b).

260

### 261 **4-2 Comparison of different fitting models**

262 As mentioned, the fitting models (bilinear, elliptical, and quadratic) have similar uncertainties, and this section  
263 compares the displacements obtained from these models. In this study, the bilinear model is used to obtain probabilistic  
264 displacements. The values of the probabilistic displacements obtained for the models (bilinear, elliptical, and  
265 quadratic) are shown in Figure 4.





266 **4-3 Annual exceedance rate of 5% in 50 years**

267 Assuming the trace of the North Tabriz fault and considering the bilinear model and the return period of 645 and 300  
268 years, the annual rate of exceedance for the two displacement scenarios of 4.5 and 7.1m has been examined.

269 In this comparison, an annual rate of exceedance of 5% in 50 years for both displacement scenarios of 4.5 and 7.1m,  
270 at distances 64 and 120m from the assumed site, has been examined in figure (5). In the case of D=4.5m, the annual  
271 rate of exceedance of D=4m at distances of 64 and 120 m for 645 years is  $1.81 \times 10^{-4}$  and  $7.51 \times 10^{-6}$  and for 300 years  
272  $2.17 \times 10^{-4}$  and  $1.32 \times 10^{-5}$  as shown in (6a). In the case of D=7.1m, the annual rate of exceedance of D= 4m at distances  
273 of 64 and 120m for 645 years is  $1.81 \times 10^{-4}$  and  $1.81 \times 10^{-4}$  and for 300 years  $1.81 \times 10^{-4}$  and  $1.81 \times 10^{-4}$  as shown in (6b).

274

275 **4-4 Probabilistic displacement of North Tabriz fault**

276 By examining the trace of the North Tabriz fault, due to the passing from the fifth region of Tabriz city, estimating  
277 the probabilistic displacement in the region is essential and predicting the areas with a higher level of hazard is an  
278 important matter. Considering a 2 km long section of the North Tabriz fault according to Figures 6, 7, and 8, the two-  
279 dimensional probabilistic displacements for the North Tabriz fault have been estimated. To estimate the probabilistic  
280 displacement, two scenarios (Mw7.7, 645years) and (Mw7.3, 300years) were considered. Figure 6 shows the  
281 probabilistic displacement of the two scenarios mentioned for the 5% exceedance rate in 50 years, by the blue color  
282 spectrum. The probabilistic displacements for the 4.5 and 7.1 m displacements for the first scenario are shown in  
283 Figures 6a and 6b, respectively, and for the second scenario, in Figures 6c and 6d, respectively. The probabilistic  
284 displacement values for the second scenario have a higher level of hazard that can be seen at greater distances from  
285 the assumed sites. The probabilistic displacement of the two scenarios for the 5% increase rate at 475 and 2475 years  
286 in Figures 7 and 8, respectively, using the blue to red color spectrum is shown.

287 Due to the lack of high magnitude instrumental earthquakes and surface ruptures, the discussion about the probabilistic  
288 failure level of this active fault is uncertain in the future. As a result, one of the ways to reduce the level of damage  
289 and financial and human losses is to avoid construction around this fault trace due to several terrible historical  
290 earthquakes.

291

292 **5 Conclusion**

293 Assuming the mechanism of strike-slip and trace of Tabriz fault as a simple trace, and considering two scenarios  
294 (Mw~7.7, 645yrs), and (Mw~7.3, 300yrs) and a fault section with a length of 50 - 60 km, the probabilistic  
295 displacement of the North Tabriz fault was estimated. Furthermore, considering the reported approach by Petersen  
296 (2011), the probabilistic displacements for an exceedance rate of 5% in 50, 475, and 2475 years for the principal  
297 probabilistic displacements (on fault) of the North Tabriz fault have been explored. The obtained results in this study  
298 can be summarized as follows.



- 299 1- We considered two scenarios according to possible displacements, return periods, and magnitudes which are  
300 reported in paleoseismic studies of the North Tabriz fault.
- 301 2- In the first scenario, possible displacement, return period and magnitude were selected between zero to 4.5;  
302 645 years and  $M_w \sim 7.7$ , respectively. In the second scenario, possible displacement, return period and  
303 magnitude were selected between zero to 7.1, 300 years, and  $M_w \sim 7.3$ , respectively.
- 304 3- For both above- mentioned scenarios, the probabilistic displacements for the rate of exceedance 5% in 50,  
305 475, and 2475 years for the principle possible displacements (on fault) of the North Tabriz fault have been  
306 estimated. For the first and second scenarios, the maximum probabilistic displacement of the North Tabriz  
307 fault at a rate of 5% in 50 years is estimated to be 186 and 230 cm.
- 308 4- Maximum displacements for 5% exceedance in 475 years and 2475 years in both return periods of 645 and  
309 300 years are estimated at 469 and 655cm.
- 310 5- In this study, the probability displacement values of the North Tabriz fault have been obtained without  
311 considering the dip, depth, and rake of the fault, which has caused the same displacement values in the north  
312 and south plane of the fault. In future studies, it is possible to investigate the geometric properties of the  
313 source producing surface rupture and reduce the recognition uncertainty in the method of probabilistic fault  
314 displacement hazard analysis.
- 315 6- The lack of large instrumental earthquakes in northwestern Iran leads to more significant epistemic  
316 uncertainty in the obtained values. Due to the passing of the North Tabriz fault through the residential area  
317 of Tabriz and destructive historical earthquakes, it is crucial to estimate the possible future displacements of  
318 this fault.

319

#### 320 **Conflicts of interests**

321 The authors declare that they have no known competing financial interests or personal relationships that  
322 could have appeared to influence the work reported in this paper.

323

#### 324 **References**

- 325 Ambraseys, N.N., and Melville, C.P.: A History of Persian Earthquakes, Cambridge University Press,  
326 England, 236, 1982.
- 327 Barka, A.: the 17 August 1999 Izmit Earthquake, *Science*, 285, 5435, 1858–1859,  
328 doi:10.1126/science.285.5435.1858, 1999.
- 329 Baize, S., Nurminen, F., Dawson, T., Takao, M., Azuma, T., Boncio, P., Marti, E.: A Worldwide and  
330 Unified Database of Surface Ruptures (SURE) for Fault Displacement Hazard Analyses, *Bull. Seismol. Soc. Am.*,  
331 499-520, <https://doi.org/10.1785/0220190144>, 2019.
- 332 Berberian, M.: Patterns of historical earthquake rupture on the Iranian plateau. In *Developments in Earth  
333 Surface Processes*, 17, <https://doi.org/10.1016/B978-0-444-63292-0.00016-8>, 2014.
- 334 Berberian, M., & Yeats, R. S.: Patterns of historical earthquake rupture in the Iranian Plateau, *Bull.  
335 Seismol. Soc. Am.*, 89, 1, 120-139, 1999.



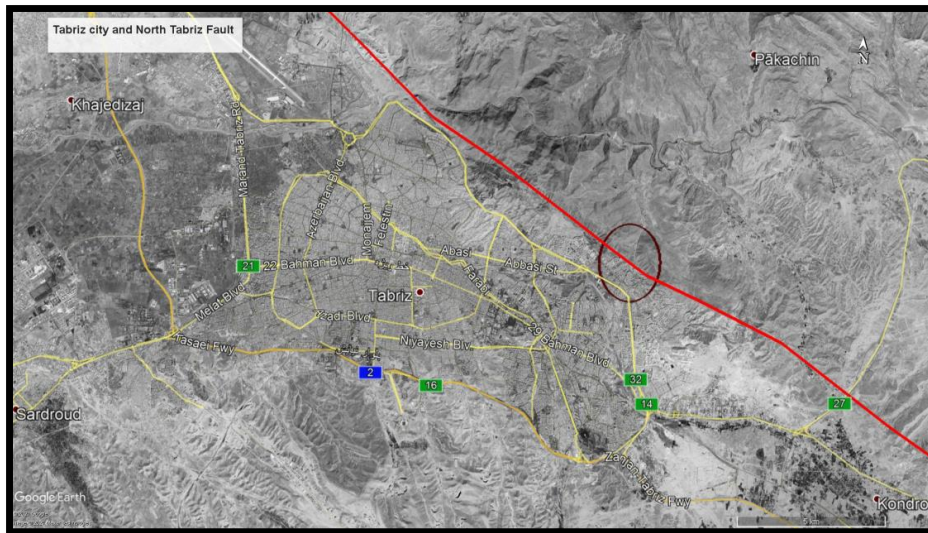
- 336 Berberian, M.: Seismic Sources of the Transcaucasian Historical Earthquakes, *Nato. Asi. 2.*, 233–311.  
337 [https://doi.org/10.1007/978-94-011-5464-2\\_13](https://doi.org/10.1007/978-94-011-5464-2_13), 1997.
- 338 Berberian, M., and Arshadi, S.: On the evidence of the youngest activity of the North Tabriz Fault and the  
339 seismicity of Tabriz city, *Geol. Surv. Iran Rep.*, 39, 397–418, 1976.
- 340 Biasi, G. P., and Weldon, R. J.: Estimating surface rupture length and magnitude of paleoearthquakes from  
341 point measurements of rupture displacement, *Bull. Seismol. Soc. Am.*, 96, 1612–1623, 2006.
- 342 Bouchon, M., Bouin, M. P., Karabulut, H., Toksöz, M. N., Dietrich, M., Rosakis, A. J.: How Fast is  
343 Rupture during an Earthquake? New Insights from the 1999 Turkey Earthquakes, *Geophys. Res. Lett.*, 28, 14, 2723–  
344 2726, 2001.
- 345 Comfort, L.: Self-Organization in Disaster Response: The Great Hanshin Earthquake of January 17, 1995,  
346 *Nat. Hazards.*, 12, 1995.
- 347 Coppersmith, K. J., & Youngs, R. R.: Data needs for probabilistic fault displacement hazard analysis, *J.*  
348 *Geodyn.*, 29, 329–343, [https://doi.org/10.1016/S0264-3707\(99\)00047-2](https://doi.org/10.1016/S0264-3707(99)00047-2), 2000.
- 349 Cornell, C. A.: Engineering seismic risk analysis, *Bull. Seismol. Soc. Am.*, 58, 5, 1583–1606,  
350 <https://doi.org/10.1785/BSSA0580051583>, 1968.
- 351 Djamour, Y., Vernant, P., Nankali, H. R., Tavakoli, F.: NW Iran-eastern Turkey present-day kinematics:  
352 Results from the Iranian permanent GPS network, *Earth. Planet. Sc. Lett.*, 307, 1–2, 27–34,  
353 <https://doi.org/10.1016/j.epsl.2011.04.029>, 2011.
- 354 Ghassemi, M. R.: Surface ruptures of the Iranian earthquakes 1900-2014: Insights for earthquake fault  
355 rupture hazards and empirical relationships, *Earth-Sci. Rev.*, 156, 1–13,  
356 <https://doi.org/10.1016/j.earscirev.2016.03.001>, 2016.
- 357 Hemphill-Haley, M. A., and Weldon II R. J.: Estimating prehistoric earthquake magnitude from point  
358 measurements of surface rupture, *Bull. Seismol. Soc. Am.*, 89, 1264–1279,  
359 <https://doi.org/10.1785/BSSA0890051264>, 1999.
- 360 Hessami, K., Pantosti, D., Tabassi, H., Shabanian, E., Abbassi, M. R., Fegghi, K., & Solaymani, S.:  
361 Paleoeearthquakes and slip rates of the North Tabriz Fault, NW Iran: Preliminary results, *Ann. Geophys-Italy.*, 46, 5,  
362 903–916, <https://doi.org/10.4401/ag-3461>, 2003.
- 363 Jennings, P. C.: Engineering features of the San Fernando earthquake of February 9, 1971, California  
364 Institute of Technology, (Unpublished), <https://resolver.caltech.edu/CaltechEERL:1971.EERL-71-02>, 1971.
- 365 Koketsu, K., Yoshida, Sh., Higashihara, H.: A fault model of the 1995 Kobe earthquake derived from the  
366 GPS data on the Akashi Kaikyo Bridge and other datasets, *Earth. Planets. Sp.*, 50, 10, 803,  
367 <https://doi.org/10.1186/BF03352173>, 1998.
- 368 Lee J. C., Chu H. T., Angelier, J., Chan Y.C., Hu J.C., Lu C.Y., Rau R.J.: Geometry and structure of  
369 northern surface ruptures of the 1999 Mw=7.6 Chi-Chi Taiwan earthquake: influence from inherited fold belt  
370 structures: *J. Struct. Geol.*, 24, 1, 173–192, [https://doi.org/10.1016/S0191-8141\(01\)00056-6](https://doi.org/10.1016/S0191-8141(01)00056-6), 2002.
- 371 Masson, F., Djamour, Y., Van Gorp, S., Chéry, J., Tatar, M., Tavakoli, F., Vernant, P.: Extension in NW  
372 Iran driven by the motion of the South Caspian Basin, *Earth. Planet. Sc. Lett.*, 252, 1–2, 180–188,  
373 <https://doi.org/10.1016/j.epsl.2006.09.038>, 2006.
- 374 Mirzaei, N., Gao, M. and Chen, Y. T.: Seismic source regionalization for seismic zoning of Iran: Major  
375 Seismotectonic provinces, *J. Earthquake. Pred. Res.*, 7, 465–495, 1998.
- 376 Moss, R. E. S., & Ross, Z. E.: 2011, Probabilistic fault displacement hazard analysis for reverse faults,  
377 *Bull. Seismol. Soc. Am.*, 101, 4, 1542–1553, <https://doi.org/10.1785/0120100248>, 2011.



- 378 Mousavi-Bafrouei, S. H., Mirzaei, N., and Shabani, E.: A declustered earthquake catalog for Iranian  
379 plateau, *Ann. Geophys-Italy.*, 57, 6, <https://doi.org/10.4401/ag-6395>, 2014.
- 380 Paul C., Rizzo Associates, I.: Probabilistic Fault Displacement Hazard Analysis Krško East and West Sites  
381 Proposed Krško 2 Nuclear Power Technical Report Probabilistic Fault Displacement Hazard Analysis Krško East  
382 and West Sites Proposed Krško 2 Nuclear Power Plant, 2013.
- 383 Petersen, M. D., and Wesnousky, S. G.: Fault slip rates and earthquake histories for active faults in  
384 southern California, *Bull. Seismol. Soc. Am.*, 84, 1608–1649, <https://doi.org/10.1785/BSSA0840051608>, 1994.
- 385 Petersen, M. D., Dawson, T. E., Chen, R., Cao, T., Wills, C. J., Schwartz, D. P., & Frankel, A. D.: Fault  
386 displacement hazard for strike-slip faults, *Bull. Seismol. Soc. Am.*, 101, 2, 805–825,  
387 <https://doi.org/10.1785/0120100035>, 2011.
- 388 Ram, T. D., & Wang, G.: Probabilistic seismic hazard analysis in Nepal: *Earthq. Eng. Eng. Vib.*, 12, 4,  
389 577–586, <https://doi.org/10.1007/s11803-013-0191-z>, 2013.
- 390 Rui, Ch., Petersen, M. D.: Improved Implementation of Rupture Location Uncertainty in Fault  
391 Displacement Hazard Assessment, *Bull. Seismol. Soc. Am.*, 109, 5, 2132–2137.  
392 <https://doi.org/10.1785/0120180305>, 2019.
- 393 Shahvar, M. P., Zare, M., and Castellaro, S.: A unified seismic catalog for the Iranian plateau (1900–  
394 2011), *Seismol. Res. Lett.*, 84, 233–249, 2013.
- 395 Stepp, J. C., Wong, I., Whitney, J., Quittmeyer, R., Abrahamson, N., Toro, G., Sullivan, T.: Probabilistic  
396 seismic hazard analyses for ground motions and fault displacement at Yucca Mountain, Nevada: *Earthq. Spectra.*,  
397 17, 1, 113–151. <https://doi.org/10.1193/1.1586169>, 2001.
- 398 Toksöz, M. N., ARPAT, E., & ŞARO&GLU, F. U. A. T.: The East Anatolian earthquake of 24 November  
399 1976, *Nature.*, 270(5636), 423–425, <https://doi.org/10.1038/270423b0>, 1977.
- 400 Wells, D. L., & Coppersmith, K. J.: New Empirical Relationships among Magnitude, Rupture Length,  
401 Rupture Width, Rupture Area, and Surface Displacement, *Bull. Seismol. Soc. Am.*, 84, 4, 974–1002,  
402 <https://doi.org/10.1785/BSSA0840040974>, 1994.
- 403 Wells, D. L., & Kulkarni, V. S.: Probabilistic fault displacement hazard analysis - Sensitivity analyses and  
404 recommended practices for developing design fault displacements, NCEE 2014 - 10th U.S. National Conference on  
405 Earthquake Engineering: Frontiers of Earthquake Engineering, October 2014, <https://doi.org/10.4231/D3599Z26K>,  
406 2014.
- 407 Wesnousky, S. G.: Displacement and geometrical characteristics of earthquake surface ruptures: Issues and  
408 implications for seismic-hazard analysis and the process of earthquake rupture, *Bull. Seismol. Soc. Am.*, 98, 4,  
409 1609–1632. <https://doi.org/10.1785/0120070111>, 2008.
- 410 Young, C. J., Lay, T., & Lynnes, C. S.: Rupture of the 4 February 1976 Guatemalan earthquake: *Bull.*  
411 *Seismol. Soc. Am.*, 79, 3, 670–689, <https://doi.org/10.1785/BSSA0790030670>, 1989.
- 412 Youngs, R. R., Arabasz, W. J., Anderson, R. E., Ramelli, A. R., Ake, J. P., Slemmons, D. B., Toro, G. R.:  
413 A methodology for probabilistic fault displacement hazard analysis (PFDHA), *Earthq. Spectra.*, 19, 1, 191–219.  
414 <https://doi.org/10.1193/1.1542891>, 2003.
- 415
- 416
- 417

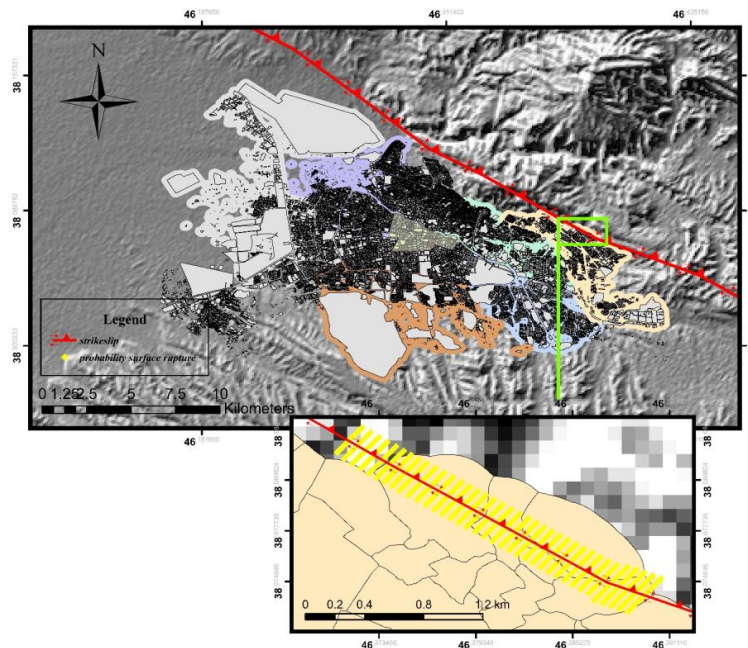


418 **List of figures:**



419  
420

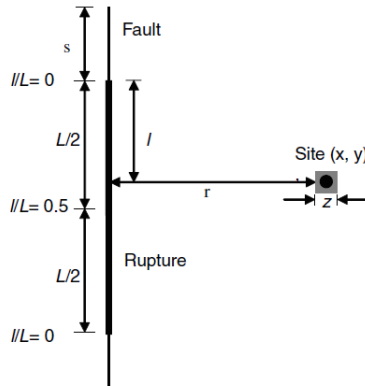
(a)



421  
422

(b)

423 Figure 1. North Tabriz Fault and Tabriz city (a), Part of the North Tabriz fault considered in this study and perpendicular profiles  
424 (b). Figure a and b are generated using Google Earth with Digital Globe imagery (© Google Earth 2021).



425

426

427

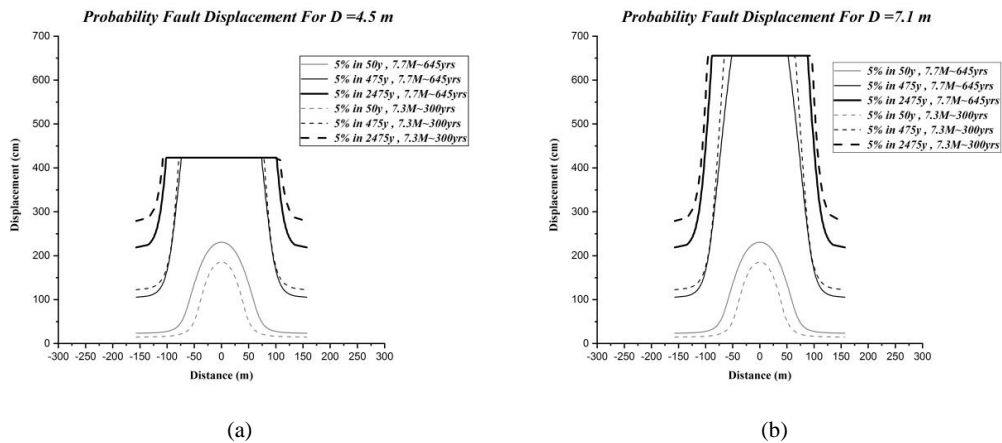
428

429

430

431

Figure 2. Definition of the variables used in fault rupture analysis:  $x$  and  $y$  Site coordinates,  $z$  Dimensions of the area intended to calculate the probability of fault rupture at the site (for example, dimensions of the building foundation),  $r$ : the distance from the site to the fault trace, ratio  $l/L$ : the distance from the fault so that  $l$  is the measured distance from the nearest point on the rupture to the nearest end of the rupture,  $L$ : the total length of the rupture and  $s$ : the distance from the end of the rupture to the end of the fault (Petersen et al., 2011).



432

433

434

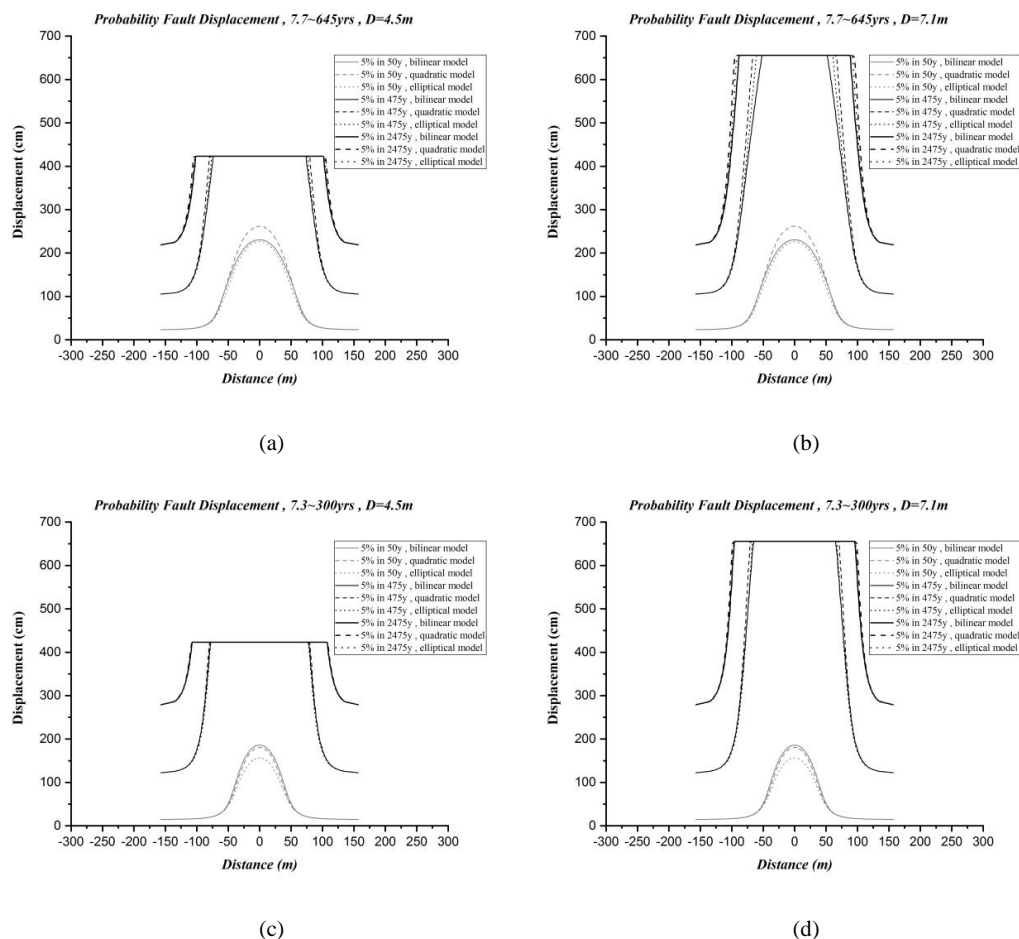
435

436

437

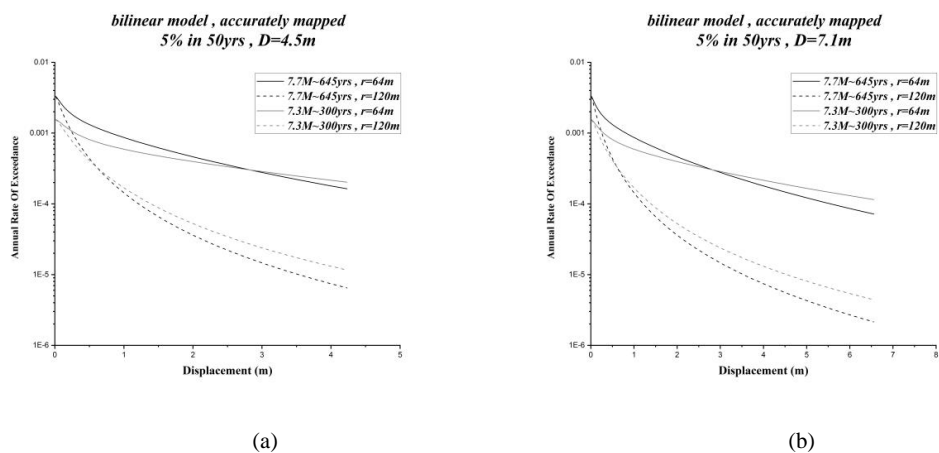
438

Figure 3. Comparison of probability displacement, 5% exceedance rate in 50, 475, and 2475 years for a)  $D=4.5$  m b)  $D=7.1$  m



439 Figure 4. Comparison of probability displacement, different fitting models for a) 645-year return period and D=4.5 m, b) 645-year return period  
440 and D= 7.1m, c) 300-year return period and 4.5 m, d) return period 300- years, and D=7.1 m

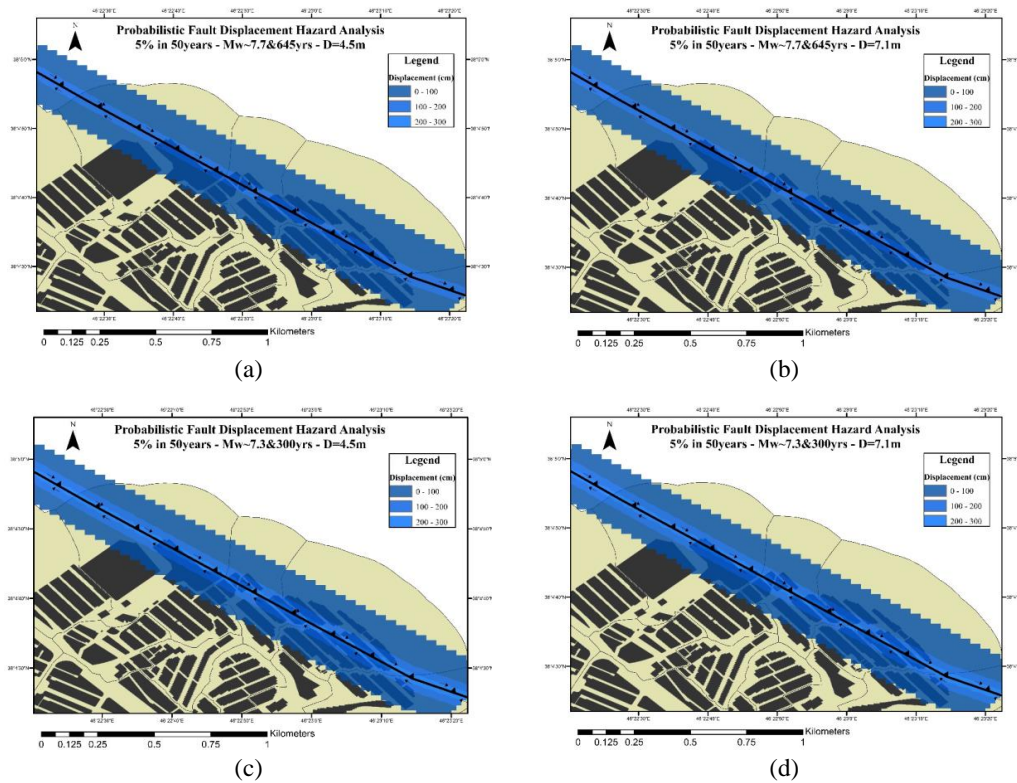
441  
442  
443  
444  
445



446 Figure 5. Comparison of the annual rate of exceedance of displacement for a) D=4.5 m displacement, b) D=7.1 m displacement

447  
448  
449  
450  
451  
452  
453  
454  
455  
456  
457  
458  
459  
460  
461  
462  
463  
464





465

466

467

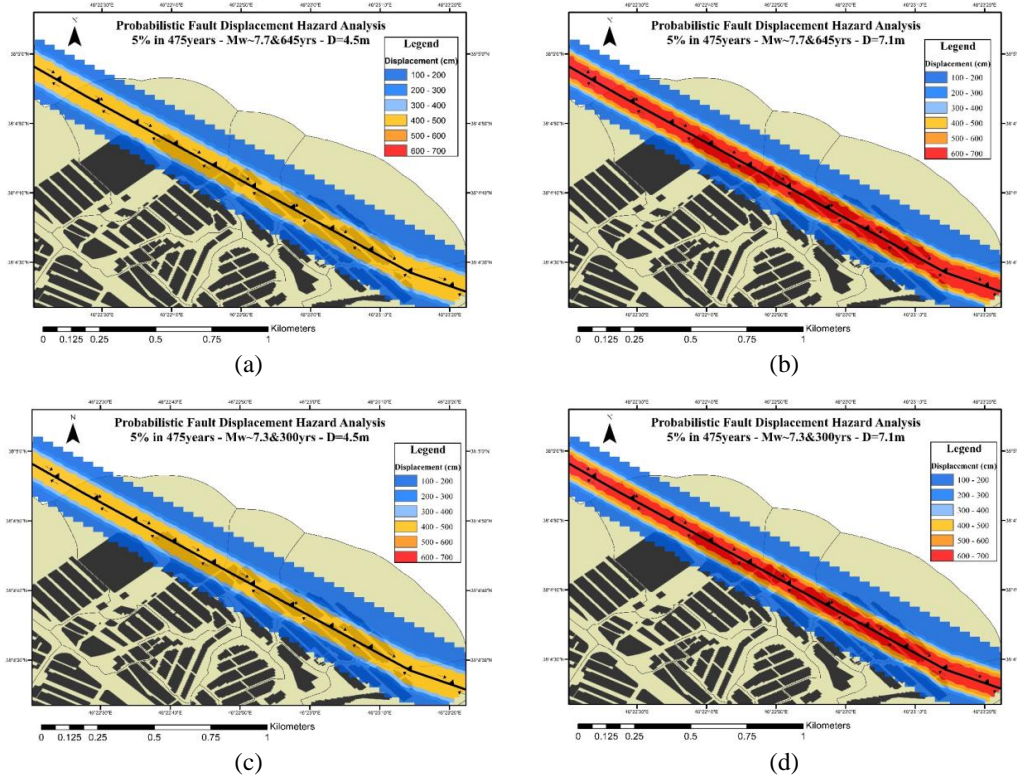
Figure 6. Probability Displacement of 5% in 50, a) Mw~7.7 and return period of 645yrs for D=4.5m, b) Mw~7.7 and return period of 645yrs for D=7.1m, c) Mw~7.3 and return period of 300yrs for D=4.5m and d) Mw~7.3 and return period of 300yrs for D=7.1m

468

469

470

471



472

473

474

Figure 7. Probability Displacement of 5% in 475, a) Mw~7.7 and return period of 645yrs for D=4.5m, b) Mw~7.7 and return period of 645yrs for D=7.1m, c) Mw~7.3 and return period of 300yrs for D=4.5m and d) Mw~7.3 and return period of 300yrs for D=7.1m

475

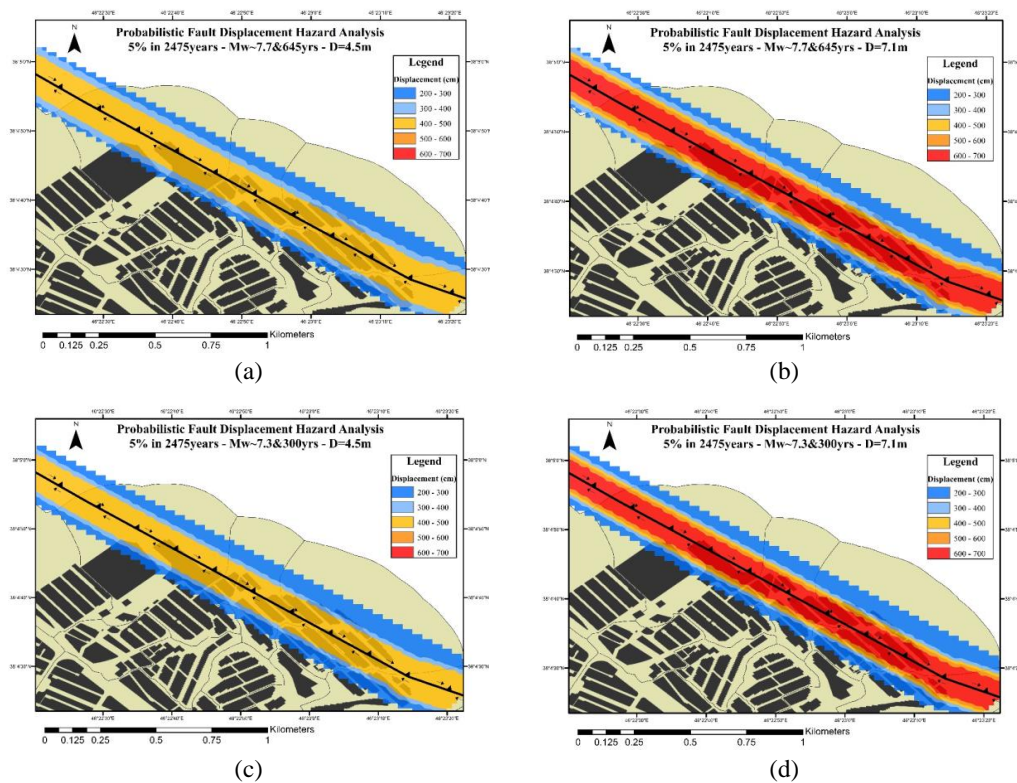
476

477

478

479

480



481

482

483

Figure 8. Probability Displacement of 5% in 2475, a) Mw~7.7 and return period of 645yrs for D=4.5m, b) Mw~7.7 and return period of 645yrs for D=7.1m, c) Mw~7.3 and return period of 300yrs for D=4.5m and d) Mw~7.3 and return period of 300yrs for D=7.1m

484

485

486

487

488

489

490

491



492 list of Tables:

493

494

Table 1. Probability of distributed rupture for different cell sizes (Petersen et al., 2011)

No.	Cell Size (m <sup>2</sup> )	a(z)	b(z)	Standard Deviation(σ)
1	25×25	-1.1470	2.1046	1.2508
2	50×50	-0.9000	0.9866	1.1470
3	100×100	-1.0114	2.5572	1.0917
4	150×150	-1.0934	3.5526	1.0188
5	200×200	-1.1538	4.2342	1.0177

499

500

501

502

503

504

505

Table 2. Summary of mapping accuracy: The measured distance from the mapped fault trace to the observed surface rupture (Petersen et al., 2011)

Mapping Accuracy	Mean (m)	One-Sided Standard Deviation (m)	Two-Sided Standard Deviation on Fault (m)
ALL	30.64	43.14	52.92
Accurate	18.47	19.54	26.89
Approximate	25.15	35.89	43.82
Concealed	39.35	52.39	65.52
Inferred	45.12	56.99	72.69

506

507

Table 3. Different Models Used in Principal Fault Attenuation Relationships (Petersen et al., 2011)

Analysis Type	Model	Weight
Multivariate	<b>BILINEAR</b> $\ln(D)=1.7969M_w+8.5206(l/L)-10.2855, \sigma_{in} = 1.2906, l/L < 0.3$ $\ln(D)=1.7658M_w-7.8962, \sigma_{in} = 0.9624, l/L \geq 0.3$	0.34
	<b>QUADRATIC</b> $\ln(D)=1.7895M_w+14.4696(l/L)-20.1723(l/L)^2-10.54512, \sigma_{in} = 1.1346$	0.33
	<b>ELLIPTICAL</b> $\ln(D)=3.3041\sqrt{1-\frac{1}{0.52}[(l/L)-0.5]^2}+1.7927M_w-11.2192, \sigma_{in} = 1.1348$	0.33

508